

Major but not minor hepatectomy accelerates engraftment of extrahepatic tumor cells

Kathrin Rupertus · Otto Kollmar · Claudia Scheuer · Bastian Junker · Michael D. Menger · Martin K. Schilling

Received: 5 July 2006 / Accepted: 8 December 2006 / Published online: 27 January 2007
© Springer Science+Business Media B.V. 2007

Abstract

Background The effect of hepatectomy and hepatic regeneration on intra- and extrahepatic tumor growth is still controversially discussed. Herein we studied the effect of minor (30%) or major (70%) hepatectomy on engraftment of extrahepatic tumor cells, and the role of tumor neovascularization and tumor cell migration.

Methods Green fluorescent protein (GFP)-transfected CT26.WT colorectal cancer cells were implanted in dorsal skinfold chambers of syngeneic BALB/c mice. Animals underwent 30% (30%Phx, $n = 8$) or 70% hepatectomy (70%Phx, $n = 8$). Sham-operated animals served as controls ($n = 8$). Angiogenesis and neovascularization as well as tumor cell migration, proliferation and growth were studied over 14 days using intravital fluorescence microscopy, histology and immunohistochemistry.

Results After both minor and major hepatectomy tumor proliferating cell nuclear antigen (PCNA) expression increased significantly ($P < 0.05$) when compared with nonhepatectomized controls. However, only major but not minor hepatectomy accelerated neovascularization ($P < 0.05$) and tumor cell migration ($P < 0.05$). This was associated with a significantly

($P < 0.05$) enhanced tumor growth after 70%Phx when compared with 30%Phx and controls. The rate of apoptotic cell death was not affected by major or minor hepatectomy.

Conclusion Regeneration after major hepatectomy accelerates extrahepatic tumor cell engraftment, most probably by acceleration of neovascularization and induction of tumor cell migration.

Keywords Colorectal cancer · Metastasis · Hepatectomy · Liver resection · Liver regeneration · Tumor growth · Microcirculation

Introduction

Colorectal cancer is the second leading cause of cancer-related mortality in the United States [1]. Death of the patients usually results from uncontrolled metastatic disease. The liver is the most common site of metastasis for colorectal cancer, and surgical resection is the only curative treatment option, as indicated by a 5-year survival up to 50% [2, 3]. Anatomic resections reduce the rate of positive margins and improve overall survival [4]. Modern surgical strategies from major hepatobiliary centers have demonstrated that hepatectomy of as much as 70% of the liver can be performed with a mortality rate of less than 5% [5–8]. Major hepatectomy has a higher complication rate compared to minor segmental liver resections, including bile leaks, abscess formation and hepatic failure [9, 10]. The extent of liver resection and the degree of baseline functional impairment are the main independent risk factors for these postoperative complications [5].

K. Rupertus · O. Kollmar (✉) · B. Junker · M. K. Schilling
Department of General, Visceral, Vascular and Pediatric Surgery, University of Saarland, 66421 Homburg/Saar, Germany
e-mail: chokol@uniklinik-saarland.de

C. Scheuer · M. D. Menger
Institute for Clinical and Experimental Surgery, University of Saarland, 66421 Homburg/Saar, Germany

Although it is well recognized, that the liver completely regenerates after major hepatectomy, the effect of hepatic regeneration on intra- and extra-hepatic tumor growth is still controversially discussed. On the one hand, experimental studies have indicated that a minor liver resection of 40% prolongs the survival of mice with diffuse colorectal liver metastasis [11]. This is probably mediated through increased interferon production by nonparenchymal liver cells [12]. On the other hand, Yokoyama and coworkers reported that minor hepatectomy (30%) accelerates growth of intrahepatically implanted hepatoma cells, and that only major hepatectomy (60%) suppresses tumor growth [13]. These findings are contrasted by the results of other experimental studies, demonstrating enhanced growth of colorectal liver metastasis after both minor (30%) [14] and major (60–70%) hepatectomy [15–18].

Similar discrepancies have been reported on the effect of hepatectomy on extrahepatic metastatic tumor growth. Ono et al. [19] observed a regression of subcutaneously implanted hepatoma cells after partial hepatectomy. In contrast, Schindel et al. [20] showed that partial hepatectomy enhances the growth of subcutaneously implanted hepatoma cells. Finally, DeJong and coworkers [15] demonstrated that neither subcapsular renal nor retroperitoneally implanted tumors increase after 70% hepatectomy.

Thus, there is no clear indication how liver regeneration after minor or major hepatectomy influences tumor growth of extrahepatic colorectal metastases. Because this knowledge is of major clinical importance, we analyzed in the present study the effect of minor (30%) and major (70%) hepatectomy on engraftment of extrahepatic tumor cells, and the role of tumor neovascularization and tumor cell migration.

Materials and methods

Tumor cell line and culture conditions

The CT26 cell line is a *N*-nitroso-*N*-methylurethane-induced undifferentiated adenocarcinoma of the colon, syngeneic with the BALB/c mouse. For our studies, the CT26.WT cell line (ATCC CRL-2638[®], LGC Promochem GmbH, Wesel, Germany) was grown in cell culture as monolayers in RPMI-1640 medium with 2 mM L-glutamine (Sigma Aldrich Chemie GmbH, Taufkirchen, Germany) supplemented with 10% fetal calf serum (FCS Gold, PAA Laboratories GmbH, Cölbe, Germany), 100 U/ml penicillin and 100 µg/ml streptomycin (PAA Laboratories GmbH). The cells were incubated at 37°C in a humidified atmosphere

containing 5% CO₂ in air. With the use of CLONfectin (Clontech, Palo Alto, California, USA) cells were transfected with the enhanced GFP expression vector pEGFP-N1 (Clontech) according to the manufacturer's instructions [21]. For the individual experiments, only CT26.WT-GFP cells of the first three serial passages after cryo-storage were used. At the day of implantation, CT26.WT-GFP cells were harvested from subconfluent cultures (70–85%) by trypsinization (0.05% Trypsin and 0.02% EDTA, PAA Laboratories GmbH), and washed twice in phosphate-buffered saline solution (PBS).

Animals

Experiments were performed after approval by the local governmental animal care committee, and conformed to the United Kingdom Co-ordinating Committee on Cancer Research (UKCCCR) Guidelines for the Welfare of Animals in Experimental Neoplasia (as described in 1998 in *Br J Cancer* 77:1–10) and the Interdisciplinary Principles and Guidelines for the Use of Animals in Research (New York Academy of Sciences Ad Hoc Committee on Animal Research, New York, USA). Twelve- to sixteen-week-old female BALB/c mice (Charles River Laboratories GmbH; Sulzfeld, Germany) with a body weight (BW) of 18–22 g were used. The animals were housed in single cages at room temperature of 22–24°C and at a relative humidity of 60–65% with a 12-h light/dark cycle environment. The mice were allowed free access to drinking water and standard laboratory chow (Altromin[®]; Lage, Germany).

Experimental model

For operative procedures, animals were anesthetized by intraperitoneal injection of 90 mg/kg BW ketamine (Ketavet[®], Parke Davis; Freiburg, Germany) and 20 mg/kg BW xylazin (Rompun[®], Bayer; Leverkusen, Germany). To allow repetitive analyses of the microcirculation of growing tumors, the dorsal skinfold chamber model was used for intravital microscopy as described previously in detail [22]. The chamber consists of two symmetrical titanium frames (weight 3.2 g), which were positioned to sandwich the extended double layer of the dorsal skin. One layer was completely removed in a circular area of 15 mm in diameter. The remaining layers, consisting of epidermis, subcutaneous tissue and striated skin muscle, were covered with a glass coverslip incorporated into one of the titanium frames [23]. The animals tolerated the chambers well and showed no signs of discomfort or changes in sleeping and feeding habits.

After a 48-h recovery period, the animals were re-anesthetized, and a 30% hepatectomy (30%Phx) or 70% hepatectomy (70%Phx) was performed. Sham-operated animals served as controls. 30%Phx included the resection of the left lateral lobe with a mean tissue weight of 0.26 ± 0.01 g. 70%Phx included the resection of the right medial, the left medial and the left lateral lobe. The mean tissue weight was 0.51 ± 0.02 g.

For tumor cell implantation, the coverslip of the chamber was temporarily removed and 1×10^5 cells were implanted onto the surface of the striated muscle tissue within the chamber. Directly after cell implantation, the chamber tissue was covered again with the coverslip [24].

Experimental protocol

A total of 24 animals received extrahepatic tumor cell implantation and were assigned to three different groups ($n = 8$ each). In the first group, animals without liver resection received tumor cell implantation and served as controls (Control). In the second group of animals 30%Phx was performed before implantation of the tumor cells. Animals of the third group received a 70%Phx before tumor cell implantation. All animals underwent repetitive intravital microscopic analyses directly as well as 5, 7, 9, 12 and 14 days after tumor cell implantation. At the end of the experiment the chamber with the tumor tissue was harvested for histology and immunohistochemistry.

Intravital fluorescence microscopy

Intravital fluorescence microscopy was performed in epi-illumination technique using a modified Zeiss Axio-Tech microscope (Zeiss, Oberkochen, Germany) with a 100-W HBO mercury lamp. Microscopic images were monitored by a charge-coupled device video camera (FK 6990, COHU, Prospective Measurements Inc., San Diego, CA) and were transferred to a video system (VO-5800 PS, Sony, München, Germany) for subsequent off-line analysis. Migration of tumor cells, tumor size, growth kinetics and angioarchitecture were analyzed using blue light epi-illumination (450–490 nm excitation wavelength and >520 nm emission wavelengths) [25].

Microcirculation analysis

Microcirculatory parameters were assessed off-line by frame-to-frame analysis of the videotaped images using a computer-assisted image analysis system (CapImage, Zeintl Software; Heidelberg, Germany). Data analysis was performed by examiners unaware of the treatment.

The fluorescent labeling of the tumor cells allowed precise delineation of the tumor from the surrounding unaffected host tissue. It also enabled for distinct identification of individual tumor cells to study tumor cell migration. At each observation time point the surface of the fluorescently labeled tumor mass within the chamber was first scanned for determination of the tumor size (given as tumor area in mm^2). Eight distinct regions of interest (ROIs) were randomly chosen next to the tumor margin, and the number of migrating tumor cells was counted within each region.

In additional eight ROIs within the tumor margin angiogenesis and neovascularization were analyzed. Angiogenesis was defined as budding, sprouting and vascular tube formation, originating from pre-existing host vessels. This was documented and scored 0–8, with 0 indicating angiogenesis in none of the ROIs and 8 indicating angiogenesis in all of the ROIs. Because it is well known that the development of functioning new vascular networks requires not only the generation of new vascular tubes, but also maturation of these blood vessels, involving the action of different growth factors and pericyte attachment, the establishment of mature functional vascular networks which presented with blood perfusion was determined as neovascularization. Neovascularization of the tumor microvasculature was measured as functional capillary density [cm/cm^2], defined as the length of newly formed red blood cell perfused capillaries per observation area, and analyzed within the eight ROIs of the tumor margin and within four additional ROIs of the tumor center. Diameters of the newly formed tumor microvessels were measured perpendicularly to the vessel path and are given in μm [21].

Histology and immunohistochemistry

At the end of the experiments (day 14), the tumor and the adjacent host tissue was harvested. For light microscopy, formalin-fixed biopsies were embedded in paraffin. Sections of $5 \mu\text{m}$ were cut and stained with hematoxylin and eosin for routine histology according to standard procedures.

To study cell proliferation and apoptotic cell death, proliferating cell nuclear antigen (PCNA) and cleaved caspase-3 were stained using indirect immunoperoxidase techniques. Therefore, deparaffinized sections were incubated with 3% H_2O_2 and 2% goat normal serum to block endogenous peroxidases and unspecific binding sites. A monoclonal mouse anti-pan PCNA antibody (PC10, 1:50; DakoCytomation, Hamburg, Germany) and a polyclonal rabbit anti-mouse cleaved caspase-3 antibody (Asp175, 1:50; Cell Signaling Technology, Frankfurt, Germany) were used as

primary antibodies. The cleaved caspase-3 antibody detects endogenous levels of the short fragment (17/19 kD) of activated caspase-3, but not full-length caspase-3. Biotinylated goat anti-mouse and goat anti-rabbit Ig antibodies were used as secondary antibodies for streptavidin–biotin–complex peroxidase staining (1:200, LSAB 2 System HRP, DakoCytomation). 3,3′ diaminobenzidine (DakoCytomation) was used as chromogen. Sections were counterstained with hemalaun and examined by light microscopy.

As a negative control, additional slices from each specimen were exposed to appropriate IgG isotype-matched antibody (Sigma Aldrich Chemie GmbH) in place of primary antibody under the same conditions to determine the specificity of antibody binding. All of the control staining was found negative.

Statistical analysis

All values are expressed as means \pm SEM. After proving the assumption of normality and homogeneity of variance across groups, differences between groups were calculated by a one-way analysis of variance (ANOVA) followed by the appropriate posthoc comparison, including correction of the alpha error according to Bonferroni probabilities to compensate

for multiple comparisons. Overall statistical significance was set at $P < 0.05$. Statistical analysis was performed with the use of the software package SigmaStat (SPSS Inc., Chicago, IL, USA).

Results

Tumor growth

The chamber implantation, the hepatectomy and the extrahepatic tumor growth did not affect the animals' general conditions during the 14-day observation period. In all groups, intravital fluorescence microscopy showed a progressive tumor growth. However, 70%Phx provoked a significant ($P < 0.05$) acceleration of tumor growth over the 14-day observation period, as indicated by an increased tumor area when compared with that measured in controls and animals, which underwent 30%Phx (Fig. 1).

Angiogenesis and neovascularization

Analysis of angiogenesis revealed ~40% of the ROIs with newly developed microvessels within the margin of the tumors at day 7. Of interest, at day 9 this ratio

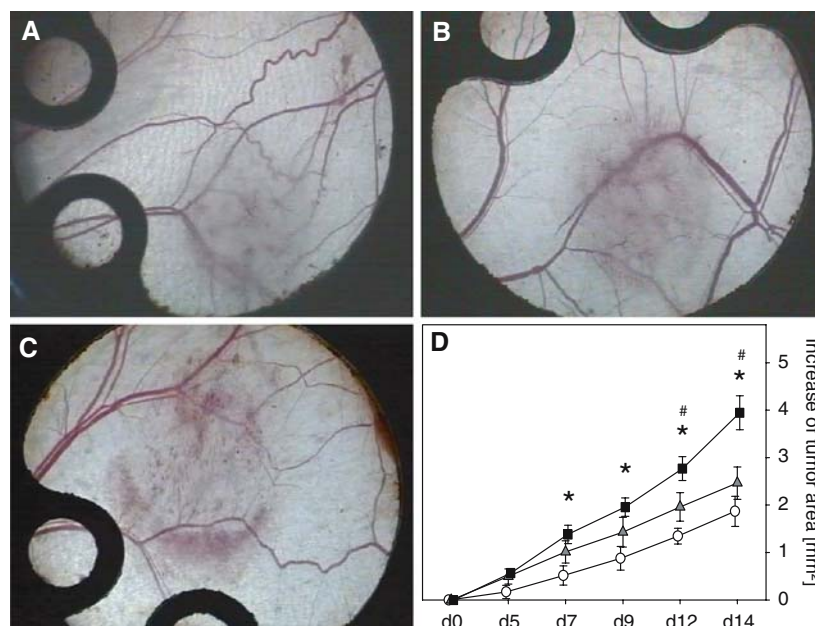


Fig. 1 Time course of tumor growth in dorsal skinfold chambers after inoculation of CT26.WT-GFP cells in BALB/c mice. Photomicrographs of representative tumors from mice which underwent sham-operation (**A**), 30% hepatectomy (**B**, 30%Phx) and 70% hepatectomy (**C**, 70%Phx) at day 14. Quantitative

analysis of the tumor area (**D**) over a 14-day period in sham-operated controls (circles) and animals, which underwent 30%Phx (triangles) and 70%Phx (squares). Note the significant increase of tumor growth after 70%Phx. Mean \pm SEM; * $P < 0.05$ versus controls; # $P < 0.05$ versus 30%Phx

amounted to ~60% in controls and 30%Phx animals, but was found increased to more than 90% after 70%Phx (Fig. 2). At day 12, almost all ROIs of the three groups demonstrated new vessel formation within the tumor margin (Fig. 2).

The vascular networks of the tumors, reflecting neovascularization, were characterized by newly developed, chaotically arranged capillaries, which were drained by large venules. The capillary density of these networks did not differ between tumor margin and tumor center (Fig. 3). Tumors of 70%Phx animals, however, developed a significantly higher ($P < 0.05$) density of newly formed tumor vessels compared to those of 30%Phx and sham controls (Fig. 3).

Because angiogenesis and neovascularization are regularly associated with vasodilation due to the action of VEGF, we analyzed the capillary diameters within the tumor vascular networks. Within all groups, the newly formed capillaries of the tumors showed significant ($P < 0.05$) dilation after hepatectomy when compared with that of controls at day 14 (data not shown). No difference of capillary dilation between tumor margin and tumor center could be observed.

Tumor cell migration

The individual CT26.WT-GFP cells could nicely be visualized without additional contrast enhancement due to their green fluorescent protein transfection (Fig. 4). High-resolution intravital fluorescence microscopy allowed a quantitative analysis of the number of cells migrating out of the tumor mass. The migrating tumor cells changed their appearance from round to a spindle-shaped phenotype and were found in a distance of 200–700 μm out of the tumor margin. Of interest, 70%Phx provoked a significant increase ($P < 0.05$) of tumor cell migration throughout the 14-day observation period when compared with 30%Phx and sham controls (Fig. 4).

Tumor cell proliferation

PCNA as an indicator of cell proliferation showed that almost 40% of the tumor cells displayed positive staining (Fig. 5). By this, the tumor sharply demarcated from the surrounding host tissue. Infiltration into host muscle could be detected in all animals involving 10–25% of the tumor length without significant

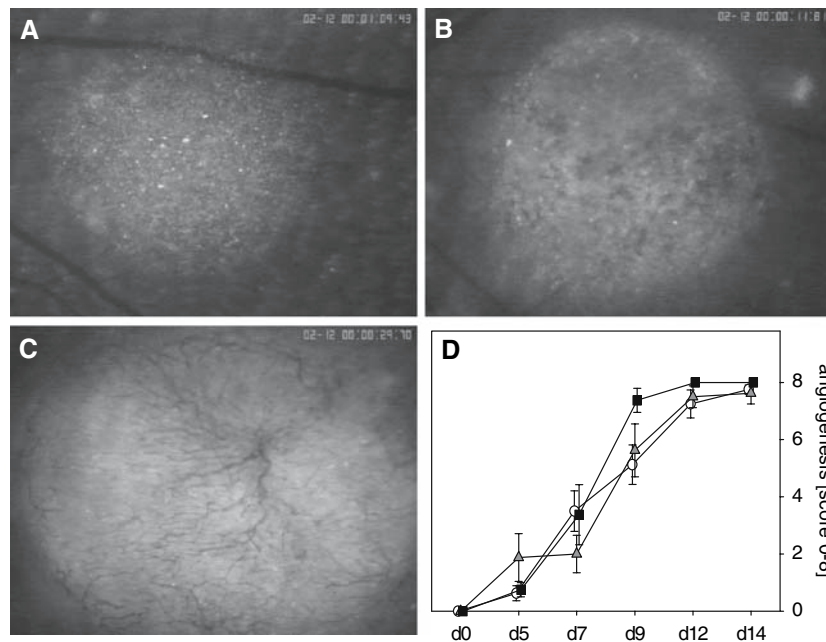
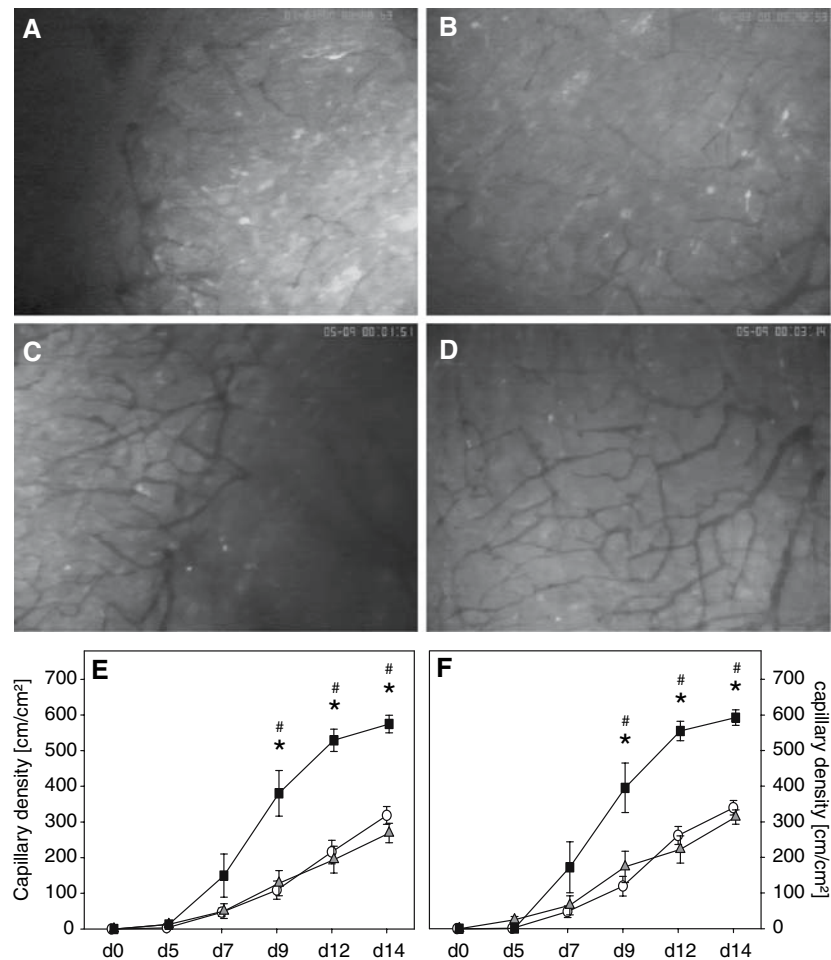


Fig. 2 Time course of the onset of angiogenesis (first signs of angiogenesis with capillary buds and sprouts) in CT26.WT-GFP tumors in dorsal skinfold chambers as determined by intravital fluorescence microscopy over a time period of 14 days. Panel **A** displays the green fluorescent protein expressing tumor cells directly after implantation in a nonhepatectomized animal (d0). Panel **B** shows the development of new blood vessels within the tumor at day 7, and panel **C** demonstrates the complete network

of newly formed microvessels at day 14. Panel **D** gives the semi-quantitative analysis of the onset of angiogenesis expressed as score from 0 to 8 (see Materials and methods) in sham-operated controls (*circles*) and animals which underwent 30%Phx (*triangles*) and 70%Phx (*squares*). Note that the onset of angiogenesis did not differ between hepatectomized animals and sham controls. Mean \pm SEM

Fig. 3 Time course of functional capillary density (neovascularization) of the tumors as determined by intravital fluorescence microscopy. The fluorescence microscopic images display the capillary network in the tumor margin (**A, C**) and the tumor center (**B, D**) of sham-operated controls (**A, B**) and 70%Phx animals (**C, D**) at day 14 after inoculation of the CT26.WT cells. By computer-assisted image analysis the capillary density of the tumor margin (**E**) and the tumor center (**F**) was analyzed in sham-operated controls (circles) and animals which underwent 30%Phx (triangles) and 70%Phx (squares). Note the significantly higher capillary density in both tumor margin and center after 70%Phx. Mean \pm SEM; * $P < 0.05$ versus controls; # $P < 0.05$ versus 30%Phx



differences between the three groups studied. Notably, 30%Phx and 70%Phx significantly ($P < 0.05$) increased the rate of PCNA-positive cells to $>60\%$ (Fig. 5), indicating an increase of tumor cell proliferation during liver regeneration after hepatectomy.

Apoptotic cell death

To study apoptotic cell death, immunohistochemistry of cleaved caspase-3 products was performed. Rarely positively stained cells could be observed in the tumors. Accordingly, quantitative analysis could not detect significant differences between the hepatectomized animals and sham-operated controls (Fig. 6).

Discussion

The major finding of the present study is that 70% hepatectomy but not 30% hepatectomy enhances neovascularization, migration and engraftment of extrahepatically implanted tumor cells.

Recent studies have indicated that surgical stress is capable of promoting tumor metastasis [26], and that hepatectomy may additionally enhance metastatic growth at extrahepatic sites [20, 26]. These observations are contrasted by the results of other reports, demonstrating a regression of extrahepatically implanted hepatoma cells after partial hepatectomy [19, 27]. In fact, de Jong and coworkers [15] demonstrated in a colon carcinoma metastasis model in the rat that major hepatectomy enhances metastatic growth in remnant livers, but not in lesions localized in the subcapsular renal and retroperitoneal space. The regulation of tumor growth after hepatectomy may differ with respect to the localization of the metastatic lesion. In line with the results of Schindel and Grosfeld [20] who showed that partial hepatectomy enhances the growth of subcutaneously implanted hepatoma cells, we demonstrate in the present study that 70% hepatectomy induces acceleration of engraftment and growth of subcutaneously implanted colon cancer metastatic lesions.

In the present study tumor cell implantation was performed at the time of hepatectomy. Accordingly,

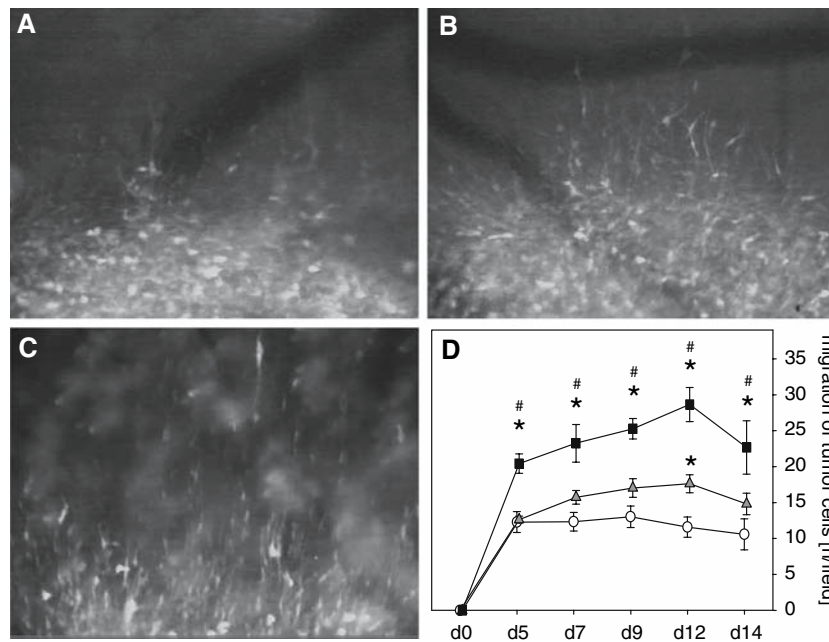
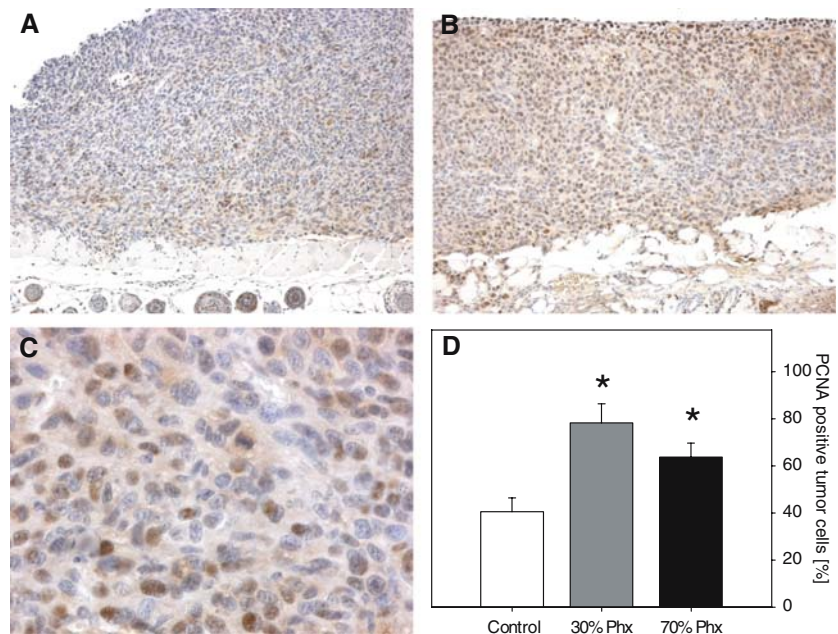


Fig. 4 Time course of tumor cell migration as determined by intravital fluorescence microscopy over a time period of 14 days. The fluorescence microscopic images display the spindle-shaped cells migrating out of the tumor margin of sham-operated controls (**A**) as well as 30%Phx (**B**) and 70%Phx (**C**) animals at day 7 after CT26.WT-GFP cell inoculation. Panel **D** demonstrates the quantitative analysis of tumor cell migration in

sham-operated controls (*circles*) and animals which underwent 30%Phx (*triangles*) and 70%Phx (*squares*). Note the significantly increased number of migrating tumor cells throughout the 14-day observation period in 70%Phx animals when compared to 30%Phx and controls. Mean \pm SEM; * $P < 0.05$ versus controls; # $P < 0.05$ versus 30%Phx

Fig. 5 PCNA immunohistochemistry of tumors of a sham-operated control (**A**) and a 70%Phx animal (**B, C**) at day 14 after CT26.WT-GFP cell inoculation. Panel **D** displays the quantitative analysis of the number of PCNA-positive cells (given in percent of all cells visible) of sham-operated controls as well as 30%Phx and 70%Phx animals. Note the significantly increased number of PCNA-positive cells after hepatectomy. Mean \pm SEM; * $P < 0.05$ versus controls



our analysis did primarily investigate tumor cell engraftment with its consequences on initial tumor growth. Similar models have been reported in the literature [14, 15, 17, 20, 26, 27]. In contrast, others have

implanted the tumors, days or weeks before hepatectomy to solely study the growth of established metastases [11, 13, 16]. In the present study, we have preferred the simultaneous implantation of tumor cells

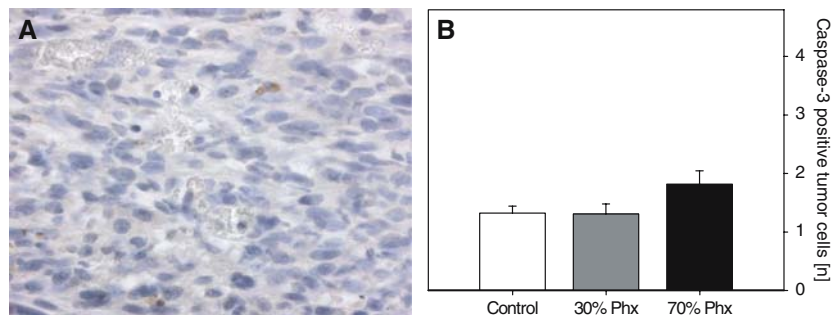


Fig. 6 Caspase-3 immunohistochemistry of a tumor of 70%Phx animal at day 14 after CT26.WT-GFP cell inoculation (**A**). Panel **B** displays the quantitative analysis of the number of caspase-3-positive cells (given per HPF) of sham-operated controls as well

as 30%Phx and 70%Phx animals. Note the almost negligible number of positively stained tumor cells in all three groups studied. Mean \pm SEM

and hepatectomy, because this may more closely mimic the clinical situation of spread of tumor cells to extrahepatic sites during liver surgery. Further, established metastases at extrahepatic sites can be diagnosed before surgery by CT, MRI and PET and resected before hepatectomy. Therefore, it is of little clinical relevance to study the influence of Phx on established metastases. In contrast nests of tumor cells, which are not engrafted, and also initially growing micrometastases with diameters <5 mm can not be detected during pre-operative diagnostics by CT, MRI and also not by PET [28, 29], and, thus, not be removed before hepatectomy. Accordingly, potential stimulation of engraftment of those tumor cells and growth of those small micrometastasis by Phx has to be considered as clinically relevant. Therefore, we herein studied tumor cell engraftment with its consequences on initial tumor growth, but not the effects of Phx on established metastases.

Surprisingly, 30% hepatectomy showed an only slight but not significant effect on extrahepatic tumor growth. This result is in contrast to findings of others, demonstrating increased growth of hepatoma cells and colorectal cancer cells in remnant livers after minor hepatectomy [13, 14]. The increased spread and growth of tumors may strongly depend on the extent of the resected liver mass. Slooter et al. and Picardo et al. have demonstrated that the growth of colorectal metastases and hepatoma cells in remnant livers after minor hepatectomy is increased without an overall increase of liver wet weight and alteration of body weight, whereas major hepatectomy resulted in excessive tumor growth with massive increase of remnant liver wet weight and pronounced alteration of the animals nutritional state [27, 30]. In line with these results, we demonstrate herein for the first time in extrahepatic tumors an only slight increase of growth

after 30% hepatectomy, but an excessive growth after 70% liver resection.

The cause of the different effect of minor versus major hepatectomy on secondary extrahepatic metastases is still unclear. It is well known that the process of angiogenesis determines the growth of metastatic lesions [31]. Previous studies have further indicated that primary tumors can inhibit angiogenesis and thus metastatic growth at secondary sites [32], and that resection of the primary tumors enhances vascularization of the secondary site metastatic lesions [32, 33]. The present study now extends this knowledge, demonstrating that the accelerated extrahepatic tumor growth after 70%Phx is associated with a significantly increased neovascularization, as indicated by an elevated microvascular density. However, the increased vascularization after 70%Phx cannot be due to the loss of a primary tumor inhibitory action on angiogenesis, because our model did not include primary hepatic tumor growth. Thus, the stimulation of vascularization in the extrahepatic tumors is most probably caused by the excessive process of liver regeneration after major hepatectomy. This view is in line with the results of an other study, which demonstrated that the hepatectomy-induced increase of tumor growth in the remnant liver can be prevented by anti-angiogenic therapy [17].

The present data show that the increase of tumor growth after major hepatectomy is not associated with an acceleration of angiogenesis, but with an enhancement of neovascularization. This is indicated by the fact that the onset of angiogenesis in the extrahepatic tumors did not differ significantly between animals, which underwent hepatectomy and sham-operated controls. In contrast, vascularization density was significantly enhanced in tumors of animals with 70% hepatectomy, indicating that major liver resection stimulates the maturation of newly formed blood

vessels and thus the establishment of tumor blood perfusion.

A considerable number of different hepatotrophic factors, which regulate the restoration of liver cell mass after hepatectomy, may contribute to the increased metastatic growth, including vascular endothelial growth factor (VEGF), hepatocyte growth factor (HGF), transforming growth factor (TGF)- α , epithelial growth factor (EGF), macrophage inflammatory protein (MIP)-2, interleukin (IL)-6, and tumor necrosis factor (TNF)- α [34]. These factors are known to induce cell migration, angiogenesis and tumor growth [17, 18, 27, 30, 35–38] and are thought to be responsible for the hepatectomy-induced increase of metastatic growth in remnant livers by paracrine action [15]. Because hepatectomy is also capable of increasing systemic levels of HGF, basic fibroblast growth factor (bFGF), VEGF and EGF [39], these factors may be responsible for the increased tumor cell migration, neovascularization and metastatic growth at extrahepatic sites.

Analysis of proliferation activity of the extrahepatic tumor cells could not detect differences at day 14 after 30 and 70% hepatectomy, although a significantly increased tumor volume after 70% Phx was observed. This indicates that the proliferative activity of the tumor cells is not the only determinant of in vivo metastatic growth. The growth of extrahepatic lesions seems to be additionally controlled by the tumor cell migrating activity. This view is supported by the fact that tumor cell migration was found significantly increased already at day 5 after major hepatectomy. Because at this time point, tumor growth did not differ significantly from that after minor hepatectomy or controls, tumor cell migration may be the cause rather than the consequence of the increased tumor growth observed at later time points.

In addition, the acceleration of neovascularization may also contribute to the significantly more pronounced metastatic growth after major compared to minor hepatectomy. In ischemic diseases, it is well known that reduced vascularization results in hypoxia, and that the nature of cell death under these conditions is shifted from apoptosis towards necrosis due to hypoxia-associated ATP depletion [40]. Accordingly, we may speculate that the lower tumor vascularization in controls and after 30% Phx may be associated with relative hypoxia, resulting in increased cell death and thus reduced tumor growth. Because the amount of apoptotic cell death did not differ between the three groups studied, the nature of cell death in these tumors has to be considered necrotic, which would be in line with that what is known from hypoxia-induced cell death in ischemic diseases.

In conclusion, we demonstrate in our mouse model that major hepatectomy stimulates engraftment and growth of extrahepatically implanted tumor cells, and that this liver regeneration-accelerated tumor growth may relate to an enhancement of neovascularization and tumor cell migration.

Acknowledgments We appreciate the excellent technical assistance of Christina Marx and Janine Becker. This study was supported by grants of the Research Committee and the Medical Faculty of the University of Saarland (HOMFOR-A/2003/1).

References

- Jemal A, Murray T, Ward E, Samuels A, Tiwari RC, Ghafoor A, Feuer EJ, Thun MJ (2005) Cancer statistics, 2005. *CA Cancer J Clin* 55:10–30
- Yamamoto J, Shimada K, Kosuge T, Yamasaki S, Sakamoto M, Fukuda H (1999) Factors influencing survival of patients undergoing hepatectomy for colorectal metastases. *Br J Surg* 86:332–337
- Fong Y, Fortner J, Sun RL, Brennan MF, Blumgart LH (1999) Clinical score for predicting recurrence after hepatic resection for metastatic colorectal cancer: analysis of 1001 consecutive cases. *Ann Surg* 230:309–318
- DeMatteo RP, Palese C, Jarnagin WR, Sun RL, Blumgart LH, Fong Y (2000) Anatomic segmental hepatic resection is superior to wedge resection as an oncologic operation for colorectal liver metastases. *J Gastrointest Surg* 4:178–184
- Imamura H, Seyama Y, Kokudo N, Maema A, Sugawara Y, Sano K, Takayama T, Makuuchi M (2003) One thousand fifty-six hepatectomies without mortality in 8 years. *Arch Surg* 138:1198–1206
- Jarnagin WR, Gonen M, Fong Y, DeMatteo RP, Ben-Porat L, Little S, Corvera C, Weber S, Blumgart LH (2002) Improvement in perioperative outcome after hepatic resection: analysis of 1803 consecutive cases over the past decade. *Ann Surg* 236:397–406
- Chang YC (2004) Low mortality major hepatectomy. *Hepatogastroenterology* 51:1766–1770
- Seyama Y, Kubota K, Sano K, Noie T, Takayama T, Kosuge T, Makuuchi M (2003) Long-term outcome of extended hemihepatectomy for hilar bile duct cancer with no mortality and high survival rate. *Ann Surg* 238:73–83
- Stewart GD, O'Suilleabhain CB, Madhavan KK, Wigmore SJ, Parks RW, Garden OJ (2004) The extent of resection influences outcome following hepatectomy for colorectal liver metastases. *Eur J Surg Oncol* 30:370–376
- Lang BH, Poon RT, Fan ST, Wong J (2003) Perioperative and long-term outcome of major hepatic resection for small solitary hepatocellular carcinoma in patients with cirrhosis. *Arch Surg* 138:1207–1213
- Castillo MH, Doerr RJ, Paolini N Jr, Cohen S, Goldrosen M (1989) Hepatectomy prolongs survival of mice with induced liver metastases. *Arch Surg* 124:167–169
- Doerr R, Castillo M, Evans P, Paolini N, Goldrosen M, Cohen SA (1989) Partial hepatectomy augments the liver's antitumor response. *Arch Surg* 124:170–174
- Yokoyama H, Goto S, Chen CL, Pan TL, Kawano K, Kitano S (2000) Major hepatic resection may suppress the growth of tumours remaining in the residual liver. *Br J Cancer* 83:1096–1101

14. Rashidi B, An Z, Sun FX, Sasson A, Gamagammi R, Moossa AR, Hoffman RM (1999) Minimal liver resection strongly stimulates the growth of human colon cancer in the liver of nude mice. *Clin Exp Metastasis* 17:497–500
15. De Jong KP, Lont HE, Bijma AM, Brouwers MA, de Vries EG, van Veen ML, Marquet RL, Slooff MJ, Terpstra OT (1995) The effect of partial hepatectomy on tumor growth in rats: in vivo and in vitro studies. *Hepatology* 22:1263–1272
16. Panis Y, Ribeiro J, Chretien Y, Nordlinger B (1992) Dormant liver metastases: an experimental study. *Br J Surg* 79:221–223
17. Drixler TA, Borel Rinkes IH, Ritchie ED, van Vroonhoven TJ, Gebbink MF, Voest EE (2000) Continuous administration of angiostatin inhibits accelerated growth of colorectal liver metastases after partial hepatectomy. *Cancer Res* 60:1761–1765
18. Delman KA, Zager JS, Bennett JJ, Malhotra S, Ebright MI, McAuliffe PF, Halterman MW, Federoff HJ, Fong Y (2002) Efficacy of multiagent herpes simplex virus amplicon-mediated immunotherapy as adjuvant treatment for experimental hepatic cancer. *Ann Surg* 236:337–342
19. Ono M, Tanaka N, Orita K (1986) Complete regression of mouse hepatoma transplanted after partial hepatectomy and the immunological mechanism of such regression. *Cancer Res* 46:5049–5053
20. Schindel DT, Grosfeld JL (1997) Hepatic resection enhances growth of residual intrahepatic and subcutaneous hepatoma, which is inhibited by octreotide. *J Pediatr Surg* 32:995–997
21. Kollmar O, Schilling MK, Menger MD (2004) Experimental liver metastasis: standards for local cell implantation to study isolated tumor growth in mice. *Clin Exp Metastasis* 21:453–460
22. Menger MD, Lehr HA (1993) Scope and perspectives of intravital microscopy-bridge over from in vitro to in vivo. *Immunol Today* 14:519–522
23. Lehr HA, Leunig M, Menger MD, Nolte D, Messmer K (1993) Dorsal skinfold chamber technique for intravital microscopy in nude mice. *Am J Pathol* 143:1055–1062
24. Menger MD, Laschke MW, Vollmar B (2002) Viewing the microcirculation through the window: some 20 years experience with the hamster dorsal skinfold chamber. *Eur Surg Res* 34:83–91
25. Vajkoczy P, Goldbrunner R, Farhadi M, Vince G, Schilling L, Tonn JC, Schmiedek P, Menger MD (1999) Glioma cell migration is associated with glioma-induced angiogenesis in vivo. *Int J Dev Neurosci* 17:557–563
26. Tsuchiya Y, Sawada S, Yoshioka I, Ohashi Y, Matsuo M, Harimaya Y, Tsukada K, Saiki I (2003) Increased surgical stress promotes tumor metastasis. *Surgery* 133:547–555
27. Picardo A, Karpoff HM, Ng B, Lee J, Brennan MF, Fong Y (1998) Partial hepatectomy accelerates local tumor growth: potential roles of local cytokine activation. *Surgery* 124:57–64
28. Stoeckli SJ, Steinert H, Pfaltz M, Schmid S (2002) Is there a role for positron emission tomography with ¹⁸F-fluorodeoxyglucose in the initial staging of nodal negative oral and oropharyngeal squamous cell carcinoma. *Head Neck* 24:345–349
29. de Jong IJ, Pruim J, Elsinga PH, Jongen MM, Mensink HJ, Vaalburg W (2002) Visualisation of bladder cancer using (11)C-choline PET: first clinical experience. *Eur J Nucl Med Mol Imaging* 29:1283–1288
30. Slooter GD, Marquet RL, Jeekel J, Ijzermans JN (1995) Tumour growth stimulation after partial hepatectomy can be reduced by treatment with tumour necrosis factor alpha. *Br J Surg* 82:129–132
31. Folkman J (2002) Role of angiogenesis in tumor growth and metastasis. *Semin Oncol* 29(Suppl 16):15–18
32. Sckell A, Safabakhsh N, Dellian M, Jain RK (1998) Primary tumor size-dependent inhibition of angiogenesis at a secondary site: an intravital microscopic study in mice. *Cancer Res* 58:5866–5869
33. Peeters CF, Westphal JR, de Waal RM, Ruiters DJ, Wobbes T, Ruers TJ (2004) Vascular density in colorectal liver metastases increases after removal of the primary tumor in human cancer patients. *Int J Cancer* 112:554–559
34. Fausto N (2000) Liver regeneration. *J Hepatol* 32:19–31
35. Kollmar O, Scheuer C, Menger MD, Schilling MK (2006) Macrophage inflammatory protein-2 promotes angiogenesis, cell migration, and tumor growth in hepatic metastasis. *Ann Surg Oncol* 13:263–275
36. Kollmar O, Menger MD, Schilling MK (2006) Macrophage inflammatory protein-2 contributes to liver resection-induced acceleration of hepatic metastatic tumor growth. *World J Gastroenterol* 12:858–867
37. Oe H, Kaido T, Mori A, Onodera H, Imamura M (2005) Hepatocyte growth factor as well as vascular endothelial growth factor gene induction effectively promotes liver regeneration after hepatectomy in Solt-Farber rats. *Hepatogastroenterology* 52:1393–1397
38. Redaelli CA, Semela D, Carrick FE, Ledermann M, Candinas D, Sauter B, Dufour JF (2004) Effect of vascular endothelial growth factor on functional recovery after hepatectomy in lean and obese mice. *J Hepatol* 40:305–312
39. Yoon SS, Kim SH, Gonen M, Heffernan NM, Detwiler KY, Jarnagin WR, D'Angelica M, Blumgart LH, Tanabe KK, Dematteo RP (2006) Profile of plasma angiogenic factors before and after hepatectomy for colorectal cancer liver metastases. *Ann Surg Oncol* 13:353–362
40. Jaeschke H, Lemasters JJ (2003) Apoptosis versus oncotic necrosis in hepatic ischemia/reperfusion injury. *Gastroenterology* 125:1246–1257